Author(s): N. A. Khovanova and I. A. Khovanov

Article Title: The role of excitations statistic and nonlinearity in energy harvesting from random impulsive excitations

Year of publication: 2011

Link to published article:
http://dx.doi.org/10.1063/1.3647556

The role of excitations statistic and nonlinearity in energy harvesting from random impulsive excitations

N. A. Khovanova[a)] and I. A. Khovanov
School of Engineering, University of Warwick, Coventry CV4 7AL, United Kingdom

Design of an efficient energy harvester is now feasible as technology develops and a viable approach to solve this need is to exploit the concept and application of a nonlinear design. In this letter, we conducted a comparative analysis of linear and nonlinear piezoelectric energy harvesting from random impulsive excitations modelled by white Poisson noise. It is shown that the harvester performance depends on both nonlinearity and properties of ambient energy, and nonlinearity should be optimized for a given type of ambient vibration in order to achieve efficient harvesting.

PACS numbers: 05.40.-a, 05.10.Ln, 05.45.-a, 84.60.-h, 88.05.-b, 88.05.Bc, 89.20.Kk
Keywords: energy harvesting, piezoelectric, ambient vibration, Poisson noise, pulses, impulsive excitation, non-Gaussian noise

Energy harvesting is a transformation of an external (ambient) energy of one type, for example, mechanical vibration or heat into an electrical form by using different transduction mechanisms for subsequent utilization[1]. The main target application of harvesting is to provide power for small scale devices by effective replacement of the traditional power supply, i.e. battery. Typically, mechanical vibrations are sources of ambient energy for such devices. The primary design of the harvesters is based on the resonant principle, aiming to a harmonic (sinusoidal) form of vibration, when a linear oscillator with a large quality factor is employed for harvesting energy[1]. Generally, harvesting efficiency should grow as $1/\omega^2$ (ω is frequency of the harmonic vibration) for a typical linear harvester[1]. Consequently, an efficiency should reach its maximum as ω tends to zero. However, for practical applications the resonant frequency is typically in the order (or more) of 100 Hz[2,3], whereas a wide range of energy sources[4] for example, human motions have low frequency vibrations (1-10 Hz). In many cases, this energy has a wide broadband and a stochastic nature[4–6]. Thus, the primary design requires modifications in order to address the spectral band limitations. Recently, introducing a nonlinearity has been suggested to overcome the limitations[7–9]. The bistable regime of harvester operation for broadband random excitations in the form of white Gaussian noise has been discussed[8,9].

The use of nonlinear design pose other challenges. It is important to take into account the features of vibration with the aim of selecting the best form of nonlinearity. The question arises whether it is sufficient only to understand the spectral context of the vibration or whether a detailed description of the vibration is a prerequisite requirement? These issues are still open and have not been adequately addressed. In this letter, we employ a model of a piezoelectric harvesting device[7–9] to analyze the role of a nonlinearity and the importance of a detailed description of vibration. We selected vibration in the form of random impulsive excitations which are described by two independent parameters (see below). The form of the impulsive excitations that can be represented by a sequence of pulses is often observed[4–6,10] and refers to impact excitations[10]. For the impacts from uncorellated sources, the impulsive excitations form random pulse train corresponding to Poisson white noise. These factors are discussed here. Also, the efficiency of the harvester with different types of nonlinearities is compared for Poisson noise excitations.

A feasibility to create different nonlinearities in piezoelectric harvesting devices by using additional magnets has been recently demonstrated. Corresponding models of devices have been validated and such models have been used to understand the outcome of the harvesters relating to harmonic signals[7,11,12] and white Gaussian noise[9]. The model under consideration here describes a ferromagnetic cantilever beam with piezoceramic layers[8,11]. It includes two parts: mechanical and electrical forming the following system

$$\begin{aligned} \ddot{x} &= -\alpha\dot{x} - \frac{dU(x)}{dx} + \chi z + f(t) \\ \dot{z} &= -\lambda z - \kappa\dot{x} \end{aligned} \tag{1}$$

The mechanical part is described by the variables x and $\dot{x}$ and this corresponds to a cantilever beam dynamics. Coordinate z corresponds to the electrical part and this is proportional to the voltage arising from the interaction between piezoceramic layers and beam bending. The extracted power is defined as:

$$P = \rho \lim_{T\to\infty} \frac{1}{T} \int_0^T z^2(t)dt, \tag{2}$$

where T is averaging time, ρ corresponds to the load conductivity[7]. For simplicity $\rho = 1$. The term $f(t)$ corresponds to an external mechanical energy source from the vibration of the beam support. We fix values of the parameters $\alpha = 0.02$, $\chi = 0.05$, $\lambda = 0.05$, $\kappa = 0.5$[8]. The term $dU(x)/dx$ describes the non-linearity of the system (1), where $U(x)$ is the magnetoelastic potential formed by permanent magnets. By changing the magnets locations

a)Electronic mail: n.khovanova@warwick.ac.uk

and/or using different numbers of magnets[7,11,12] $U(x)$ can be varied consequently changing the system nonlinearity. However, it is unclear as to how the potential shape and this system nonlinearity influence energy harvesting. In order to address this question, let us consider several types of $U(x)$ with distinct shapes:

$$U_L(x) = x^2/2, \quad U_B(x) = -x^2/4 + x^4/2,$$
$$U_F(x) = x^4, \quad U_M(x) = x^2/2 + x^4/2$$

where indices L, B, F and M correspond to linear, bistable, flat and monostable potentials, respectively. Note that U_L is realized in the absence of magnets. The system (1) with linear, bistable and monostable potentials has the same resonant frequency $\omega_0 \approx 1.0124$ for weak vibration, whereas for the flat potential $\omega_0 = 0$.

To compare the performance of (1) for different potential shapes we introduce an efficiency index in the following form

$$\gamma = 10 \log 10 \left(\frac{P_N}{P_L} \right), \tag{3}$$

where P_L is the power (2) for the linear case, P_N represents the power (2) for different nonlinear potentials. The results for γ are given in dB units. For the input signals as considered below, the output power P_L is a linear function of the input power, P_{in}, that results in a constant ratio $P_L/P_{in} = C$ (C = constant). Numerical simulations of (1) were performed in order to obtain values of γ. The simulations used the Heun methods for stochastic differential equations[13] with corresponding modifications for Poisson noise[14]. After a relaxation period $T_r = 10^7$, the power P was calculated for a finite $T = 10^{10}$. The zero initial conditions $x = 0$, $\dot{x} = 0$ and $z = 0$ were used to mimic corresponding experimental setup[9].

The linear potential U_L is an optimal shape for a harmonic signal $f(t) = A\sin(\omega_0 t)$, and a nonlinear design cannot significantly improve the performance[12]. Indeed, for weak signal (A is small) the efficiency of the system (1) with bistable and monostable potentials is close to the linear case since they are characterized by the same resonant frequency ω_0. The growth of A induces a nonlinear response and the efficiency decreases[12]. Since the resonant frequency is zero for the flat potential significantly poorer efficiency for $U_F(x)$ is expected than for the case of $U_L(x)$. However the scenario can change when a different form of ambient energy is involved.

Let us then consider the signal $f(t)$ in the form of Poisson white noise[15] which represents a sequence of independent pulses

$$f(t) = \sum_i^N \lambda \delta(t - t_i), \tag{4}$$

where λ is pulse amplitude, t_i are independent random times of the pulse appearance. Time intervals $\tau_i = t_{i+1} - t_i$ between two subsequent pulses has exponential distribution, with the parameter Λ and a number

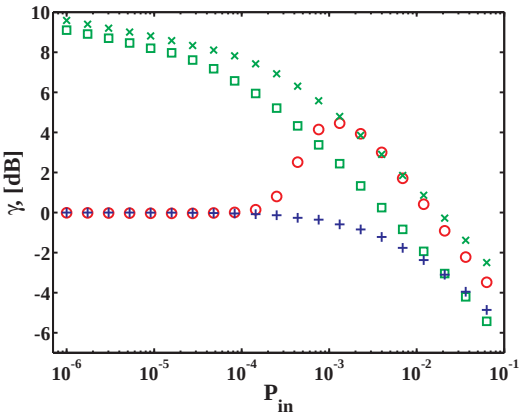

FIG. 1. The efficiency γ as a function of the input power $P_{in} = \lambda^2\Lambda$ of Poisson noise for bistable, $U_B(x)$, (marker ○), monostable, $U_M(x)$, (marker +) and flat , $U_F(x)$, (marker □) and $U_{FF}(x)$, (marker ×) potentials.

of pulses, n, for time interval, δt, and obeys the Poisson distribution

$$p(n) = \frac{(\delta t \Lambda)^n \exp(-\delta t \Lambda)}{n!}. \tag{5}$$

The parameter Λ defines the frequency of the pulse appearance. Since pulses are independent the resulting spectrum is white. The input power of Poisson noise is $P_{in} = \lambda^2\Lambda$ and the noise induces a constant bias $I = \lambda\Lambda$. In the limit of $1/I \to 0$ (while P_{in} is constant) Poisson noise can be substituted by Gaussian noise. By varying the bias I for a fixed P_{in} the shape of the Poisson distribution (5) changes from symmetrical (close to Gaussian, when $1/I \to 0$), to a strongly asymmetrical non-Gaussian shape ($1/I \to \infty$). The value of $1/I$ can therefore be considered as a parameter of the asymmetry of distribution (5).

Let us now consider γ as a function of the input power, $P_{in} = \lambda^2\Lambda$ for variation in λ and the fixed value of $\Lambda = 1$ (Fig. 1)[16]. The flat potential demonstrates the best performance for weak input power. In this case, the system (1) performs oscillations near an equilibrium state and nonlinear potentials can be replaced by corresponding linear potentials. For flat potential $\omega_0 = 0$; this leads to an efficient transformation of lower frequency components of the Poisson noise with $1/\omega^2$ scaling. The response of (1) for $U_B(x)$ and $U_M(x)$ potentials coincides with the linear case since they are characterized by the same ω_0. The growth of P_{in} induces larger amplitudes of oscillations, and the response becomes correspondingly nonlinear. As a result, the efficiency, γ, decreases for $U_M(x)$ and $U_F(x)$ with increase of λ. In the bistable case, there are noise-induced jumps between states of $U_B(x)$ starting with a given value of λ, leading to enhanced efficiency. Further increase of λ leads to a decrease in γ for $U_B(x)$, which indicates that γ has an extremum. For both potentials $U_F(x)$ and $U_B(x)$ the efficiency is greatly improved than for the linear case, for a wide range of P_{in},

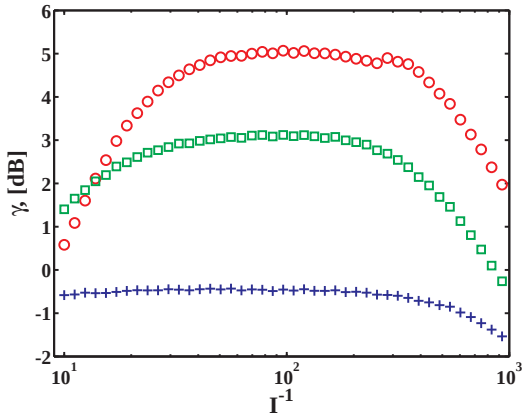

FIG. 2. The efficiency γ as a function of the inverse bias $1/I$ for bistable (marker $\circ$), monostable (marker $+$) and flat (marker $\square$) potentials.

whereas this is not the case for $U_M(x)$.

For moderate and strong P_{in} the bistable potential shows better performance than $U_F(x)$, although the flat potential shows the best performance for a weak input signal $f(t)$. For the latter, noise induced oscillations occur near an equilibrium state where the potential is maximally flat, i.e. $\partial^2 U/\partial x^2 = 0$. The extension of this maximally flat region should therefore lead to an improvement of the performance for higher P_{in}. This conclusion is validated by the consideration of $U_{FF} = x^4/4$ (marker $\times$ in Fig. 1), for which the efficiency γ is larger than for the bistable potential in the entire range of P_{in}.

The influence of the assymetry of noise distribution has been investigated where the input power is fixed $P_{in} = \lambda^2\Lambda = 0.001$, and the bias I is varying as shown in Fig. (2). It is to be noted here that P_L changes weakly with I and is nearly a constant. The efficiency γ is negative and decreases monotonically with $1/I$ for $U_M(x)$. In contrast, γ shows a non-monotonic behaviour for both $U_F(x)$ and $U_B(x)$ with a maximal efficiency γ in between the two limits $1/I \to 0$ and $1/I \to \infty$. Thus, γ depends nonlinearly on statistical characteristics of Poisson noise. Although similar parametric dependences are observed for the flat and bistable potentials, underlying mechanisms are different. For the flat case, the performance is maximal when pulses are rare enough to be processed as a single pulse, having the low-frequency spectral content. Since the response for $U_F(x)$ is larger in the low-frequency region, harvesting is efficient. More frequent pulses shift an effective frequency content to the high frequency region leading to decrease of the power; additionally the bias I changes the flatness of the potential. The other limit ($1/I \to \infty$) of rare pulses with a large amplitude leads to the power decrease as well since the pulses induce deviations far away from the flat area of $U_F(x)$. In the bistable case, the performance is defined by a frequency of jumps between the states. For small values of $1/I$, the bias I increases the barrier between the states and the output power decreases. In the opposite region of large values of $1/I$, the probability of jumps also decreases due to a nonlinear dependence of the jump probability on I[17]. As a result, there is a region of $1/I$ with a maximal performance.

In conclusion, the in-depth comparison of the linear and several nonlinear potentials and related analysis as presented here, show that the efficiency of energy harvesting is strongly dependant on the properties of ambient vibrations. The efficiency of the harvester with the flat potential changes from an inferior state for a harmonic signal to the best (if $U_{FF}(x)$ is selected) for the random impulsive excitation. A good performance can be observed in the bistable case for harvesting impulsive excitations. The results (Fig. 2) demonstrate a nontrivial dependence of efficiency of the harvesters on statistical properties of random excitations viz whilst the input power remains constant the output power can change over a wide range of values depending on the symmetry of the distribution of the amplitude of the excitations. This conclusion strongly suggests that in order to design an efficient harvester, it is vitally important to take into account a comprehensive description of properties of the ambient vibrations.

The work has been supported by EPSRC (EP/C53932X/2).

[1] K. A. Cook-Chennault, N. Thambi, and A. M. Sastry, Smart Mater. Struct. **17** (2008).
[2] S. R. Anton and H. A. Sodano, Smart Mater. Struct. **16**, R1 (2007).
[3] L. Gu and C. Livermore, Smart Mater. Struct. **20**, 045004 (2011).
[4] R. Clough and J. Penzien, *Dynamics of Structures*, 2nd ed. (Mcgraw-Hill, New York; London, 1993).
[5] J. Solnes, *Stochastic Processes and Random Vibrations: Theory and Practice* (John Wiley & Sons, Chichester, U.K.; New York, 1997).
[6] Y. Lin and G. Cai, *Probabilistic Structural Dynamics: Advanced Theory and Applications*, 2nd ed. (Mcgraw-Hill, New York; London, 2004).
[7] A. Erturk, J. Hoffmann, and D. J. Inman, Appl. Phys. Lett. **94** (2009).
[8] G. Litak, M. Friswell, and S. Adhikari, Appl. Phys. Lett. **96**, 214103 (2010).
[9] F. Cottone, H. Vocca, and L. Gammaitoni, Phys. Rev. Lett. **102** (2009).
[10] R. Ibrahim, *Vibro-Impact Dynamics* (Springer-Verlag, Berlin; Heidelberg, 2009).
[11] S. C. Stanton, C. C. McGehee, and B. P. Mann, Appl. Phys. Lett. **95** (2009).
[12] A. Triplett and D. D. Quinn, J. Intell. Mater. Syst. Struct. **20**, 1959 (2009).
[13] I. A. Khovanov, Phys. Rev. E **77**, 011124 (2008).
[14] B. Huard, H. Pothier, N. O. Birge, D. Esteve, X. Waintal, and J. Ankerhold, Ann. Phys.-Berlin **16**, 736 (2007).
[15] C. Van Den Broeck, J. Stat. Phys. **31**, 467 (1983).
[16] Qualitatively similar results were observed for varying Λ and fixed λ.
[17] I.A. Khovanov and T. Novotny, unpublished.